

Surfactant Mediated Control of Pore Size and Morphology for Molecularly Ordered Ethylene-Bridged Periodic Mesoporous Organosilica

Yongde Xia and Robert Mokaya*

School of Chemistry, University of Nottingham, University Park, Nottingham, U.K. NG7 2RD

Received: September 29, 2005; In Final Form: January 11, 2006

A series of ethylene-containing mesoporous organosilica materials were fabricated via surfactant-mediated assembly of 1,2-bis(triethoxysilyl)ethylene (BTEE) organosilica precursor using alkyltrimethylammonium bromide (C_n TAB) surfactants with different alkyl chain length ($n = 12, 14, 16, 18$) as supramolecular templates. The presence of molecularly ordered ethylene groups in the resulting periodic mesoporous organosilica (PMO) materials was confirmed by XRD data along with ^{29}Si and ^{13}C MAS NMR analysis. Additional characterization techniques, namely nitrogen sorption, TEM, and TGA, confirmed the structural ordering and thermal stability of the molecularly ordered ethylene-bridged PMOs. The PMOs exhibit molecular-scale ordering (with a periodicity of 5.6 Å) within the organosilica framework and tunable pore size, which depending on the alkyl chain length of the surfactant templates, varied in the range 23–41 Å. Furthermore, depending on the alkyl chain length of the templates, the particle morphology of the PMOs gradually changed from monodisperse spheres (for C_{12} TAB) to rod or cakelike particles (for C_{14} TAB) and elongated ropelike particles for longer chain surfactants. Variations in the surfactant chain length therefore allowed control of both the pore size and particle morphology without compromising molecular-scale or structural ordering. The reactivity of ethylene groups was probed by bromination, which demonstrated the potential for further functionalization of the PMOs.

1. Introduction

The extension of surfactant-templated self-assembly to organic-bridged silsesquioxane $(\text{RO})_3\text{Si}-\text{R}'-\text{Si}(\text{OR})_3$ species has ushered in a new materials chemistry research field.^{1–6} The resulting periodic mesoporous organosilica (PMO) materials, which are prepared via surfactant mediated condensation of organosilica precursors that possess two trialkoxysilyl groups connected by an organic bridge, represent a new family of nanoporous organic/inorganic materials that present novel and attractive properties compared to their inorganic periodic mesoporous silica (i.e., M41S type) counterparts.^{1–6} The organic groups in PMOs are uniformly distributed both within the pore wall framework and on the pore channel surface; every Si atom is connected to one (or more) C atom(s) via Si–C bonds. These unique characteristics afford specific properties to the PMOs, namely, higher organic loading and greater avoidance of pore blockage, organic groups that constitute an integral part of the mesoporous framework and greater variability in the nature of the organic groups thus offering flexibility in the properties of the materials and opportunities for further chemical functionalization (of organic groups). PMOs are therefore potentially useful as hosts for nanocluster synthesis, optoelectronic materials, shape-selective catalysts, chemical sensors, nanoreactors, and low- k microelectronic packing materials.^{1–6} Ever since the first reports on PMOs in 1999,^{7–9} much effort has been devoted to the fabrication of materials that incorporate a variety of organic groups.^{1,2} So far a range of organic groups have been incorporated into the pore walls of PMOs, including simple alkane chains, unsaturated ethylene or aromatic groups and thiophene groups.^{10–21} Interconnected three-ring $[\text{Si}(\text{CH}_2)]_3$, bridged trimethylcyclic, dendrimer, and even large heterocyclic groups have also been successfully introduced into PMOs.^{22–25}

In general, most PMOs possess good mesostructural ordering but lack local molecular-scale ordering. However, in some cases, mesoporous organosilicas with semicrystalline pore walls may be obtained by choice of organic bridging group and synthesis conditions; the crystallinity arises from molecular-scale ordering of the organic groups within the pore walls. Inagaki and co-workers were the first to report the synthesis of phenyl-bridged mesoporous organosilicas that exhibit molecular-scale ordering in the pore wall with a periodicity of 7.6 Å.^{16,26} Subsequently, biphenyl- and allyl-containing PMOs have also been shown to exhibit molecular-scale periodicity in their pore walls; π – π stacking of the bridging functional groups is claimed to contribute to the molecular-scale periodicity.^{11,13,17} Recently, Sayari and Wang reported the synthesis of a PMO material from an organosilica precursor containing both aromatic and olefinic functional groups;¹⁰ this material exhibited a structural periodicity with a spacing of 11.9 Å due to the formation of lamellar bis(ethen-2-yl)benzene silica within the pore walls. To date, the majority of molecularly ordered mesoporous organosilicas have been prepared from aromatic-based (i.e., phenyl- or biphenyl-containing) organosilica precursors.^{10,11,13,16,17,26} However, we have very recently extended semicrystalline pore wall ordering to organosilicas that do not contain aromatic bridging groups by preparing ethylene-bridged mesoporous organosilicas that exhibit molecular-scale ordering (with a periodicity of 5.6 Å) in the pore walls.²⁷

To meet the requirements of PMO applications where specific pore diameters are needed, it is necessary to control the pore size of the materials. It is well-known that the pore size of mesoporous silica can be tuned using surfactants with different chain lengths.^{28,29} In general, large pore materials may be obtained from high molecular weight surfactants (triblock copolymers) while low molecular weight surfactants (alkylammonium ions) yield materials with smaller pores. However, there

* Corresponding author. E-mail: r.mokaya@nottingham.ac.uk.

are very few reports on control of pore diameter in PMO materials.^{30,31} Sayari and co-workers synthesized a series of ethane-bridged PMOs with pore size ranging from 29 to 44 Å using C10–C18 alkyltrimethylammonium bromide as templates.³⁰ Rocha and co-workers synthesized benzene-bridged PMOs using C14 to C18 alkyltrimethylammonium bromide as surfactants;³¹ the resulting materials exhibited molecular-scale periodicity and pore diameters tunable from 32 to 39 Å. In addition to controlling the pore size of PMOs, surfactants with varying chain length can modify the hydrophobicity/hydrophilicity of the synthesis gel,³² and therefore, they significantly influence the morphology of the materials.

Ethylene-bridged PMO materials^{7,9,27,33–35} are attractive due to the presence of unsaturated ethylene groups that offer opportunities for further chemical functionalization of the organosilica frameworks.³⁶ Indeed ethylene is a well-known active group which can be readily subjected to various chemical modifications.^{7,9,18,34,36} Ethylene-bridged PMOs may be prepared in acid media using poly(ethylene oxide) polymers as surfactants.³³ In general such materials do not exhibit any molecular-scale periodicity.³³ Ethylene-bridged PMOs may also be prepared from basic synthesis media.^{7,9,27,34,35} However, so far, only cetyltrimethylammonium bromide has been used as template, and molecular-scale periodicity in the pore walls is only achieved under specific synthesis conditions.²⁷ The synthesis of molecularly ordered ethylene-bridged PMOs with variable pore size remains a desirable research goal. Apart from textural properties, the morphology of mesoporous organosilicas is an important factor in their use as catalysts, molecular sieves or in the fabrication of materials for advanced applications.^{1–6} Here we report on our attempts to control the morphology, pore size, and molecular scale ordering in mesoporous organosilicas. We have used alkylammonium surfactants of varying alkyl chain length to prepare molecularly ordered ethylene-bridged mesoporous organosilicas. The use of alkylammonium surfactants of varying alkyl chain length enables the simultaneous control of both pore size and morphology. We show that the molecular scale periodicity is not affected by the changes in pore size and morphology and that a proportion of the molecularly ordered ethylene groups are accessible to further reaction.

2. Experimental Section

2.1. Material Synthesis. 1,2-Bis(triethoxysilyl)ethylene (BTEE) was synthesized following an established procedure.³⁷ Only the distilled fraction with boiling point higher than 90 °C/15 µmHg was used as organosilica precursor. The typical procedure for the synthesis of PMOs was as follows: calculated amount of alkyltrimethylammonium bromide (C_n TAB, $n = 14, 16, 18$) was dissolved in 64.87 g of distilled water under stirring, followed by addition of 0.96 g of NaOH to control the pH. Then, 3.52 g of 1,2-bis(triethoxysilyl)ethylene was added to the mixture under stirring to give a mixture of molar ratio 1 BTEE to 1.2 C_n TAB to 2.4 NaOH to 360 H₂O. After continuous stirring for 20 h at room temperature, the synthesis mixture was transferred to an autoclave and aged at 100 °C for 24 h. The autoclave was then cooled to room temperature and the solid product obtained by filtration and repeatedly washed with a large amount of distilled water. After air-drying at room temperature, the dry (as-synthesized) material was subjected to refluxing in an ethanol solution containing 4 wt % HCl for 2 h to extract the surfactant. The solvent extraction procedure was repeated three times to ensure complete removal of the surfactant. The mesoporous organosilica materials obtained from C₁₄TAB, C₁₆TAB, and C₁₈TAB surfactants were labeled as EHOI–C14, EHOI–C16 and EHOI–C18, respectively. To synthesize mesoporous organo-

silica using dodecyltrimethylammonium bromide (C₁₂TAB), a mixture of molar composition 1 BTEE to 1.2 C₁₂TAB to 2.0 NaOH to 360 H₂O was used. All the other procedures were as described above, and the resulting material was designated as EHOI–C12.

2.2. Bromination Reaction. The reactivity of ethylene groups was probed using the bromination reaction as follows: 0.2 g of surfactant-free organosilica material was predried at 100 °C for several hours and loaded into a small glass vial, which was placed in a glass beaker. Several drops of bromine were added to the beaker, avoiding direct contact with the organosilica sample in the vial. The beaker was covered with Parafilm to contain the bromine gas and the sample exposed to bromine for a period of 24 h at room temperature. The brominated sample (orange in color) was then washed with dichloromethane (CH₂Cl₂), followed by further washing with a large amount of water and ethanol. The color of the product changed from orange to white during the washing procedure, implying removal of any physisorbed bromine.

2.3. Materials Characterization. Powder X-ray diffraction (XRD) analysis was performed using a Philips 1830 powder diffractometer with Cu K α radiation (40 kV, 40 mA), 0.02° step size, and 2 s step time. Nitrogen sorption isotherms and textural properties of the materials were determined at –196 °C using nitrogen in a conventional volumetric technique by a Micromeritics ASAP 2020 sorptometer. Before analysis the samples were oven dried at 150 °C and evacuated for 12 h at 200 °C under vacuum. The surface area was calculated using the BET method based on adsorption data in the partial pressure (P/P_0) range 0.05 to 0.2 and total pore volume was determined from the amount of the nitrogen adsorbed at $P/P_0 = \text{ca. } 0.99$. Thermogravimetric analysis (TGA) was performed using a Perkin-Elmer Pyris 6 TGA analyzer with a heating rate of 10 °C/min under static air conditions. Elemental composition was obtained using a CHNS analyzer (Fisons EA 1108). Transmission electron microscopy (TEM) images were recorded on a JEOL 2000-FX electron microscope operating at 200 kV. Samples for analysis were prepared by spreading them on a holey carbon film supported on a grid. Scanning electron microscopy (SEM) images were recorded using a JEOL JSM-820 scanning electron microscope. Samples were mounted using a conductive carbon double-sided sticky tape. A thin (ca. 10 nm) coating of gold sputter was deposited onto the samples to reduce the effects of charging. ²⁹Si and ¹³C magic angle spinning (MAS) nuclear magnetic resonance (NMR) spectra were acquired at room temperature using a 7.5 mm probe on a Varian Unity Inova 300 MHz spectrometer at the EPSRC Solid-State NMR Service (Durham). ²⁹Si spectra were obtained with a silicon-29 frequency of 59.55 MHz, spectral width of 30 kHz, acquisition time of 30 ms, and a MAS rate of 5.1 kHz. ¹³C spectra were obtained at a frequency of 75.39 MHz, spectral width of 30 kHz with acquisition time of 20 ms, and MAS rate of 5.0 kHz. ²⁹Si and ¹³C signals were referenced to tetramethylsilane (TMS).

3. Results and Discussion

3.1. Physicochemical Characterization. The XRD patterns of surfactant-free organosilica materials shown in Figure 1 are typical for mesostructured MCM-41 type materials with moderate to high structural ordering. In all cases the low angle region of the XRD patterns exhibit a basal (100) diffraction peak at 2θ between 2 and 2.6°. The position of the basal (100) peak shifts to lower 2θ values (i.e., basal spacing increases) for organosilicas templated by longer chain surfactants. The changes in basal spacing are summarized in Table 1; the spacing

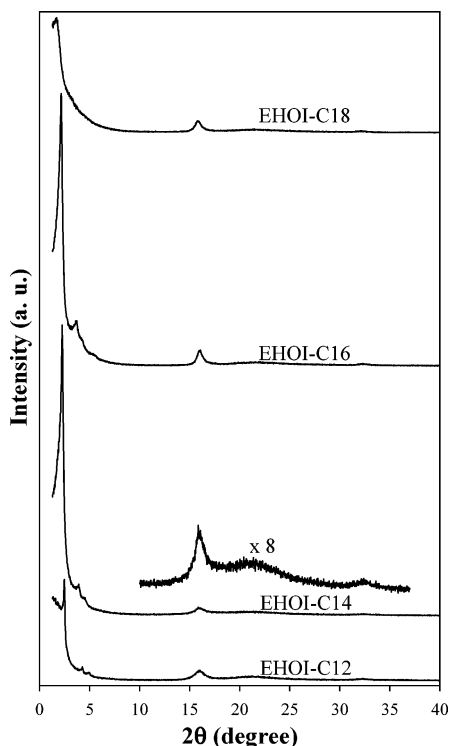


Figure 1. Powder XRD patterns of mesoporous organosilica materials prepared using various surfactants. See Experimental Section for sample designation.

TABLE 1: Textural Properties of Surfactant-Free Ethylene-Containing Periodic Mesoporous Organosilica Materials

sample	d_{100} spacing (Å)	surface area ($\text{m}^2 \text{g}^{-1}$)	pore vol ($\text{cm}^3 \text{g}^{-1}$)	pore size ^a (Å)
EHOI-C12	35.7	952	0.90	23.7
brominated-C12	36.2	775	0.70	21.0
EHOI-C14	39.0	1125	1.08	30.1
EHOI-C16	42.1	1182	1.05	36.6
brominated-C16	42.4	871	0.80	35.4
EHOI-C18	45.3	1205	1.04	40.7

^a Average pore size calculated using BJH analysis of the nitrogen adsorption isotherm.

gradually increases with the alkyl chain length of the template. The increase in basal spacing is relatively uniform and occurs in steps of ca. 3.2 Å as the alkyl chain length increases (by steps of two carbon atoms) from C₁₂ to C₁₈. A similar stepwise increase (4.2 Å per two carbon atoms in surfactant chain length) in basal spacing of benzene-bridged PMOs has been reported by Rocha and co-workers.³¹ In addition to the basal peak, the low angle region of the XRD patterns for C₁₂TAB-, C₁₄TAB-, and C₁₆TAB-templated samples display several well-resolved peaks in the 2θ range of 3–6°, which indicate that these materials are well-ordered periodic mesoporous organosilicas with *P6mm* hexagonal structures.^{28,29} The C₁₈TAB-templated sample, which exhibits only the basal peak in the low angle region of the RXD pattern, appears to have a lower level of hexagonal pore channel ordering. The XRD patterns of all the PMOs also display peaks in the wide angle region (at 2θ of 16.5 and 33.2°), which may be assigned to molecular-scale ordering of the ethylene groups within the organosilica framework. The wide angle peaks, which correspond to a basal spacing of 5.6 Å, confirm the presence of homogeneously distributed ethylene groups that exhibit molecular-level periodicity in the framework.²⁷

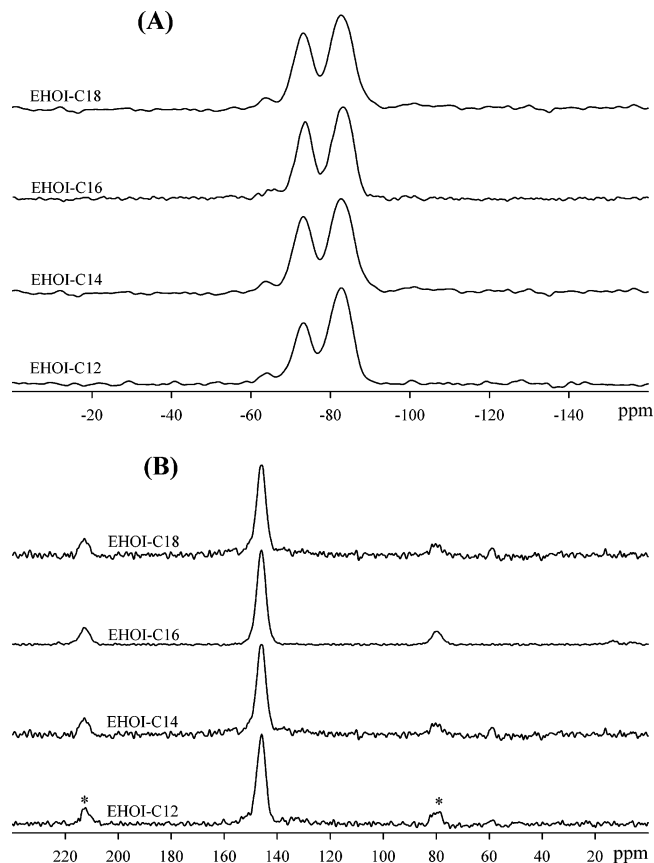


Figure 2. ²⁹Si MAS NMR (A) and ¹³C MAS NMR (B) spectra of molecularly ordered mesoporous organosilica materials prepared using various surfactants. (An asterisk denotes a spinning sideband.)

²⁹Si and ¹³C MAS NMR are useful tools for probing the presence of ethylene groups in PMO materials. The ²⁹Si and ¹³C MAS NMR spectra for surfactant-free materials are shown in Figure 2. The ²⁹Si MAS NMR spectra for all the PMOs (Figure 2A) exclusively exhibit three main signals at −64, −75, and −83 ppm, which can be assigned to silicon bonded to carbon, i.e., T¹ [C–SiO(OH)₂], T² [C–SiO₂(OH)], and T³ [C–SiO₃] respectively. The relative intensity of the Tⁿ peaks suggests that a significant proportion (> 95%) of the Si in the organosilica materials is in the T² or T³ environment, and all the samples have similar T³/(T² + T¹) ratios, implying a similar level of silica network condensation for all the PMOs. The fact that no peaks in the range of −90 to −115 ppm can be observed indicates that there was no silicon–carbon cleavage (i.e., Qⁿ [(Si(OSi)_n(OH)_{4−n}], *n* = 2–4) was not formed) during the synthesis process. The ¹³C NMR spectrum for all the ethylene-bridged mesoporous materials (Figure 2B) exhibits a main peak at ca. 146 ppm, which is due to ethylene functional groups linked to silicon. The small peaks at 58 and 18 ppm are from residual ethanol solvent.²⁷ The absence of peaks in the range of 10–30 ppm suggests that virtually all the surfactant was removed from the organosilica materials during the extraction process.

The nitrogen sorption isotherms of the ethylene-bridged organosilica materials are presented in Figure 3 and corresponding textural properties are summarized in Table 1. All the organosilica materials exhibit type IV isotherms with a typical capillary condensation step into mesopores in the partial pressure (*P/P*₀) range of 0.25–0.6. The nitrogen sorption isotherms are therefore consistent with the XRD patterns in Figure 1 and confirm that the materials possess good mesostructural ordering. All the isotherms exhibit hysteresis (type H2) due to network effects commonly observed for this type of material.^{38,39} It is

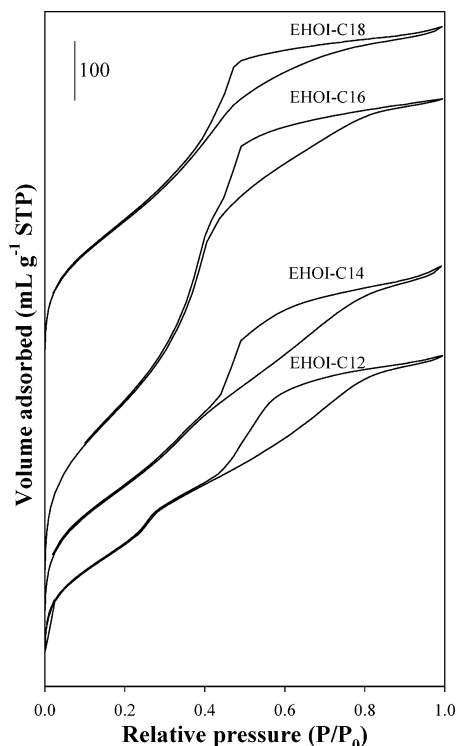


Figure 3. Nitrogen sorption isotherms of mesoporous organosilica materials prepared using various surfactants.

noticeable that although the PMOs exhibit similar nitrogen sorption isotherms, the capillary condensation step (of the adsorption isotherm) shifts to higher partial pressure for materials prepared from longer chain surfactants. This shift implies an increase of pore size (Table 1) and is in agreement with the expansion in basal spacing (and lattice parameter a_0) observed from the XRD patterns in Figure 1. The average pore size estimated from BJH analysis of the adsorption branch of the isotherms increases from 23 to 41 Å with increase in the chain length of the surfactant from C₁₂TAB to C₁₈TAB. The pore size distribution curves in Figure 4 (and Supporting Figure 1S) indicate that all the organosilica materials have relatively narrow pore size distribution; sample EHOI-C12, prepared from C₁₂TAB has a slight hint of bimodal size distribution with a small proportion of larger (>40 Å) pores. Nevertheless, pore size distribution curves plotted over a wider pore size range (shown in Supporting Figure 1S) do not indicate the presence of a significant proportion of larger (i.e., >40 Å) pores. We note that the adsorption rather than desorption branch of the isotherms was used to calculate the pore size distribution so as to avoid ambiguities arising from tensile strength effects, which are known to occur at P/P_0 of between 0.4 and 0.5 for nitrogen at 77 K.^{38,39} The surface area (>950 m²/g) and pore volume (>0.9 cm³/g) of the PMOs are typical for well-ordered MCM-41 type materials. Representative TEM images presented in Figure 5 further confirm that the PMOs possess well-ordered pore channels; it is possible to observe ordered pore channels which run throughout the particles or at the edge of particles as shown in Figure 5. The pore size estimated from the TEM images is 25 and 37 Å for sample EHOI-C12 and EHOI-C16, respectively. These estimates are very close to the average pore size calculated from the nitrogen sorption data (Table 1), and they are consistent with the pore size distribution maxima in Figure 4.

The thermal stability of the ethylene-containing mesoporous organosilica materials was evaluated by thermogravimetric analysis (TGA). As shown in Figure 6, all the surfactant-free

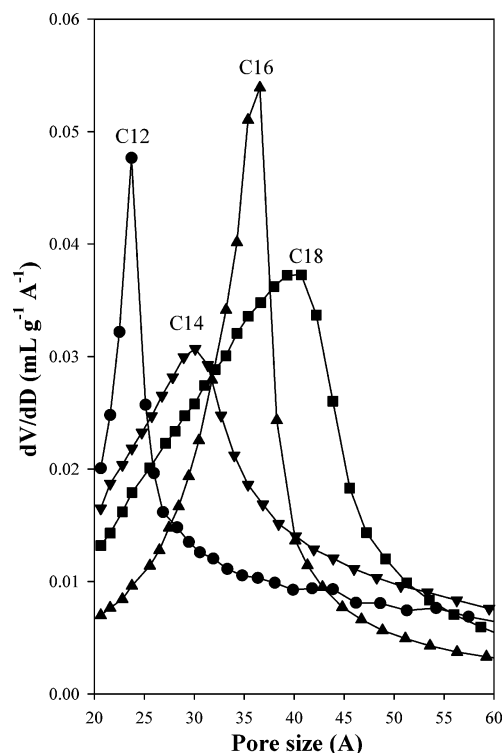


Figure 4. Pore size distribution for mesoporous organosilica materials prepared using various surfactants.

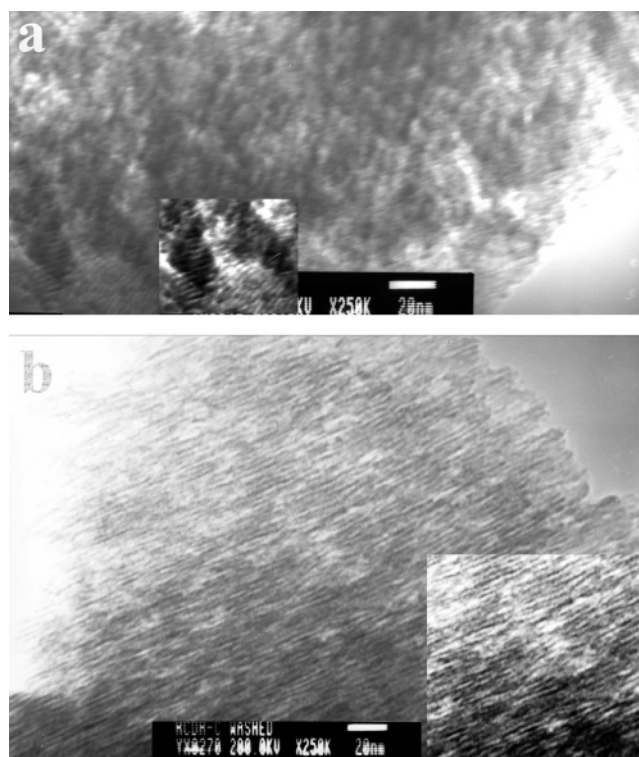


Figure 5. Representative TEM images for surfactant-free ethylene-containing mesoporous organosilica materials: (a) EHOI-C12 and (b) EHOI-C16.

ethylene-bridged PMOs exhibit ca. 5 wt % loss (water or residual ethanol) below 120 °C and a further 15% weight loss between 300 and 750 °C, which we attribute to the decomposition of ethylene groups in the inorganic–organic framework. This suggests that, regardless of the surfactant used as template, the ethylene groups in all the PMOs are stable up to 300 °C, which is in agreement with previous reports.^{27,35}

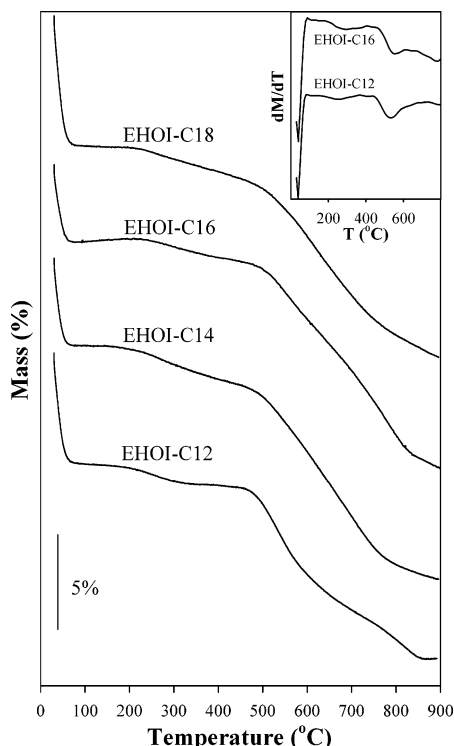


Figure 6. Thermogravimetric analysis curves of surfactant-free ethylene-containing mesoporous organosilica materials prepared using various surfactants. The inset shows DTG profiles.

The particle morphology of the PMOs was probed by scanning electron microscopy (SEM) and representative images for various samples are presented in Figure 7. The sample synthesized from C₁₂TAB surfactant exclusively exhibits spherical particle morphology (Figure 7a). The spheres have smooth surface (Supporting Figure 2Sa) and size typically in the range 5–9 μm . Virtually all the spheres are free-standing without aggregation. For C₁₄TAB-templated PMOs, the particle morphology is dominated by elongated particles with rough surfaces

(Figure 7b and Supporting Figure 2Sb) that appear to be made up of smaller spherical particles. However, virtually no isolated small spherical particles are observed. Templating with C₁₆TAB yields long ropelike particles of length between 30 and 60 μm (Figure 7c). The ropelike particles appear to be made up of smaller rodlike particles. In some cases the smaller rodlike particles pack into cake-shaped particles (Supporting Figure 2Sc) of diameter between 3 and 6 μm . Templating with C₁₈TAB also yields long ropelike particles with sharp edges (Figure 7d). The overall effect of increasing the alkyl chain length of the surfactants is a gradual change of particle morphology from spheres to elongated ropelike particles. It is therefore possible to control both the particle morphology and pore size of the present molecularly ordered PMOs by simply changing the alkyl chain length of the templating surfactants.

3.2. Reactivity of Molecularly Ordered Ethylene Groups. Functionalization of the C=C Bond. To evaluate the accessibility of ethylene groups in the mesoporous organosilica materials, bromination experiments were performed on samples EHOI-C12 and EHOI-C16. First we note that the pore channel ordering for brominated samples was generally comparable to that of the starting PMOs (Supporting Figure 3SA). However the peak at 2θ of 16.5°, which is due to the molecular-scale periodicity of ethylene groups in the framework, was significantly reduced for brominated samples due presumably to the reaction of ethylene groups with bromine to form C–Br bonds. The bromination had no significant effect on mesostructural ordering (Supporting Figure 3SB) but caused a decrease of pore diameter and ca. 20% reduction in surface area and pore volume (Table 1). Bromination did not alter the particle morphology of the ethylene-bridged mesoporous organosilica materials (Supporting Figure 4S). Furthermore, bromination had no influence on the Si environments as shown by the ²⁹Si NMR spectrum of brominated samples in Figure 8A, although the T³/T² ratio was increased for the brominated samples. The ¹³C NMR spectrum of brominated samples exhibits a peak at ca. 33 ppm (Figure 8B), which is attributable to the formation of C–Br bonds after the bromination reaction.^{9,33–35} This peak confirms that some of the ethylene groups in the mesoporous

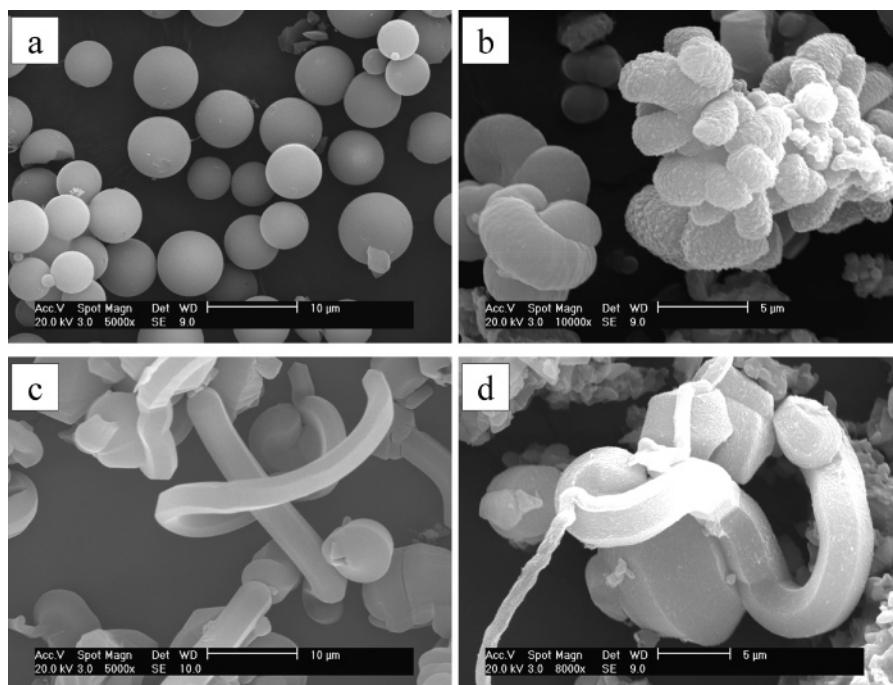


Figure 7. Representative SEM images of mesoporous organosilica materials obtained from various surfactants: (a) EHOI-C12, (b) EHOI-C14, (c) EHOI-C16, and (d) EHOI-C18.

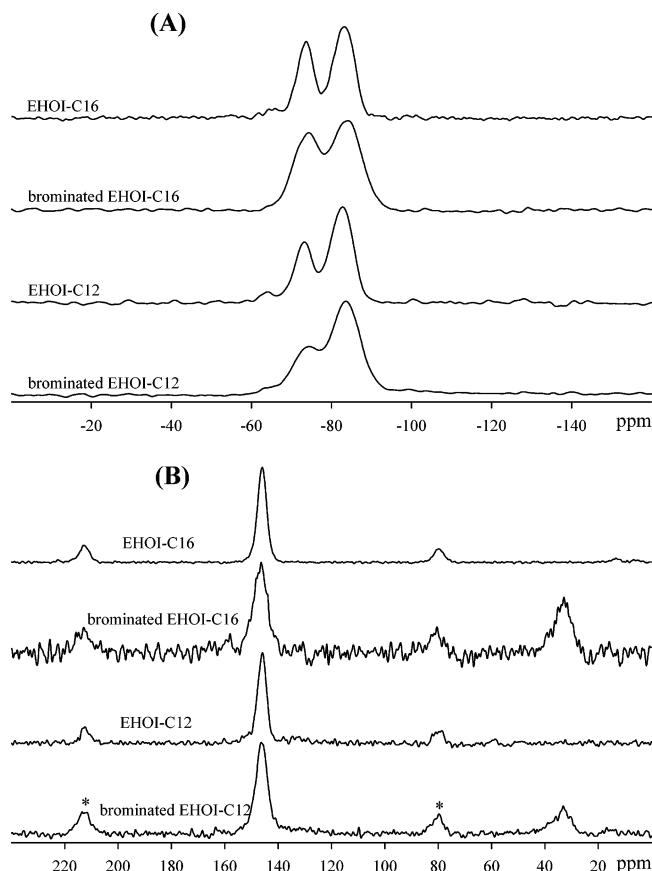


Figure 8. ^{29}Si MAS NMR (A) and ^{13}C MAS NMR (B) spectra of molecularly ordered mesoporous organosilica materials before and after bromination. (An asterisk denotes a spinning sideband.)

organosilica materials are accessible to functionalization. The peak at ca. 146 ppm, which is due to the presence of ethylene groups in the framework, is retained in the brominated samples, suggesting that not all the ethylene groups reacted with the bromine. On the basis of elemental analysis of the brominated samples, we estimate that ca. 35% of ethylene groups in the organosilica samples reacted with bromine under our bromination conditions.

4. Conclusions

We have shown that morphology, pore size, and molecular scale ordering in ethylene-bridged periodic mesoporous organosilicas (PMOs) may be readily controlled by choice of the alkylammonium surfactants used as templates. The use of alkylammonium surfactants (C_nTAB) of varying alkyl chain length ($n = 12, 14, 16, 18$) enables the simultaneous control of both pore size and morphology of the PMOs. Depending on the alkyl chain length of the surfactant templates, the pore size may be varied in the range 23–41 Å. The particle morphology of the PMOs may also be controlled to monodisperse spheres (for C_{12}TAB), rodlike or cakelike particles (for C_{14}TAB), or elongated ropelike particles for longer chain surfactants. We have shown that the molecular scale periodicity is not affected by the changes in pore size and morphology and that a proportion of the molecularly ordered ethylene groups are accessible to further reaction.

Acknowledgment. The authors are grateful to the University of Nottingham and the EPSRC for financial support and thank Dr. David Apperley at the EPSRC Solid State NMR service (Durham) for the NMR spectra.

Supporting Information Available: Four additional figures, showing pore size distribution curves of mesoporous organosilica materials over a wider pore size range, SEM images of mesoporous organosilica materials obtained from various surfactants, powder XRD patterns and nitrogen sorption isotherms of mesoporous organosilica materials before and after bromination, and SEM images of brominated mesoporous organosilica samples. This material is available free of charge via the Internet at <http://pubs.acs.org>.

References and Notes

- (1) Hatton, B.; Landskron, K.; Whitnall, W.; Perovic, D.; Ozin, G. A. *Acc. Chem. Res.* **2005**, *38*, 305.
- (2) Kickelbick, G. *Angew. Chem., Int. Ed.* **2004**, *43*, 3102.
- (3) Sanchez, C.; Lebeau, B.; Chaput, F.; Boilot, J. P. *Adv. Mater.* **2003**, *15*, 1969.
- (4) Wight, A. P.; Davis, M. E. *Chem. Rev.* **2002**, *102*, 3589.
- (5) Sayari, A.; Hamoudi, S. *Chem. Mater.* **2001**, *13*, 3151.
- (6) Stein, A.; Melde, B. J.; Schroden, R. C. *Adv. Mater.* **2000**, *12*, 1403.
- (7) Asefa, T.; MacLachlan, M. J.; Coombs, N.; Ozin, G. A. *Nature (London)* **1999**, *402*, 867.
- (8) Inagaki, S.; Guan, S.; Fukushima, Y.; Ohsuna, T.; Terasaki, O. *J. Am. Chem. Soc.* **1999**, *121*, 9611.
- (9) Melde, B. J.; Holland, B. T.; Blanford, C. F.; Stein, A. *Chem. Mater.* **1999**, *11*, 3302.
- (10) Sayari, A.; Wang, W. *J. Am. Chem. Soc.* **2005**, *127*, 12194.
- (11) Kapoor, M. P.; Inagaki, S.; Ikeda, S.; Kakiuchi, K.; Suda, M.; Shimada, T. *J. Am. Chem. Soc.* **2005**, *127*, 8174.
- (12) Morell, J.; Wolter, G.; Froba, M. *Chem. Mater.* **2005**, *17*, 804.
- (13) Kapoor, M. P.; Yang, Q.; Inagaki, S. *Chem. Mater.* **2004**, *16*, 1209.
- (14) Kapoor, M. P.; Inagaki, S. *Chem. Lett.* **2004**, *33*, 88.
- (15) Wang, W.; Zhou, W.; Sayari, A. *Chem. Mater.* **2003**, *15*, 4886.
- (16) Inagaki, S.; Guan, S.; Ohsuna, T.; Terasaki, O. *Nature (London)* **2002**, *416*, 304.
- (17) Kapoor, M. P.; Yang, Q.; Inagaki, S. *J. Am. Chem. Soc.* **2002**, *124*, 15176.
- (18) Asefa, T.; Kruk, M.; MacLachlan, M. J.; Coombs, N.; Grondy, H.; Jaroniec, M.; Ozin, G. A. *J. Am. Chem. Soc.* **2001**, *123*, 8520.
- (19) Dag, O.; Yoshina-Ishii, C.; Asefa, T.; MacLachlan, M. J.; Grondy, H.; Coombs, N.; Ozin, G. A. *Adv. Funct. Mater.* **2001**, *11*, 213.
- (20) Lu, Y.; Fan, H.; Doke, N.; Loy, D. A.; Assink, R. A.; LaVan, D. A.; Brinker, C. J. *J. Am. Chem. Soc.* **2000**, *122*, 5258.
- (21) Guan, S.; Inagaki, S.; Ohsuna, T.; Terasaki, O. *J. Am. Chem. Soc.* **2000**, *122*, 5660.
- (22) Olkhoviyk, O.; Jaroniec, M. *J. Am. Chem. Soc.* **2005**, *127*, 60.
- (23) Landskron, K.; Ozin, G. A. *Angew. Chem., Int. Ed.* **2005**, *44*, 2107.
- (24) Landskron, K.; Ozin, G. A. *Science* **2004**, *306*, 1529.
- (25) Landskron, K.; Hatton, B. D.; Perovic, D. D.; Ozin, G. A. *Science* **2003**, *302*, 266.
- (26) Yang, Q.; Kapoor, M. P.; Inagaki, S. *J. Am. Chem. Soc.* **2002**, *124*, 9694.
- (27) (a) Xia, Y. D.; Wang, W. X.; Mokaya, R. *J. Am. Chem. Soc.* **2005**, *127*, 790. (b) Xia, Y. D.; Mokaya, R. *J. Mater. Chem.* **2006**, *16*, 395.
- (28) Beck, J. S.; Vartuli, J. C.; Roth, W. J.; Leonowicz, M. E.; Kresge, C. T.; Schmitt, K. D.; Chu, C. T. W.; Olson, D. H.; Sheppard, E. W.; McCullen, S. B.; Higgins, J. B.; Schlenker, J. L. *J. Am. Chem. Soc.* **1992**, *114*, 10834.
- (29) Kresge, C. T.; Leonowicz, M. E.; Roth, W. J.; Vartuli, J. C.; Beck, J. S. *Nature (London)* **1992**, *359*, 710.
- (30) Hamoudi, S.; Yang, Y.; Moudrakovski, I. L.; Lang, S.; Sayari, A. *J. Phys. Chem. B* **2001**, *105*, 9118.
- (31) Bion, N.; Ferreira, P.; Valente, A.; Goncalves, I. S.; Rocha, J. *J. Mater. Chem.* **2003**, *13*, 1910.
- (32) Chen, C. N.; Lin, H. P.; Tsai, C. P.; Tang, C. Y. *Chem. Lett.* **2004**, *33*, 838.
- (33) Wang, W.; Xie, S.; Zhou, W.; Sayari, A. *Chem. Mater.* **2004**, *16*, 1756.
- (34) Xia, Y.; Mokaya, R. *Microporous Mesoporous Mater.* **2005**, *86*, 231.
- (35) Nakajima, K.; Lu, D.; Kondo, J. N.; Tomita, I.; Inagaki, S.; Hara, M.; Hayashi, S.; Domen, K. *Chem. Lett.* **2003**, *32*, 950.
- (36) Lim, M. H.; Blanford, C. F.; Stein, A. *J. Am. Chem. Soc.* **1997**, *119*, 4090.
- (37) Loy, D. A.; Carpenter, J. P.; Yamanaka, S. A.; McClain, M. D.; Greaves, J.; Hobson, S.; Shea, K. J. *Chem. Mater.* **1998**, *10*, 4129.
- (38) Kruk, M.; Jaroniec, M. *Chem. Mater.* **2001**, *13*, 3169.
- (39) Tompsett, G. A.; Krogh, L.; Griffin, D. W.; Conner, W. C. *Langmuir* **2005**, *21*, 8214.